The Route to Negative Thermal Expansion in ZrW_2O_8

D. Cao*, F. Bridges, G. R. Kowach, A. P. Ramirez

D. Cao and F. Bridges. Department of Physics, UCSC, Santa Cruz, CA 95064, USA

G. R. Kowach, Agere Systems, 600 Mountain Avenue, Murray Hill, NJ 07974

A. P. Ramirez, MS-K764, Los Alamos National Laboratory, Los Alamos, NM 87545

*E-mail address: dcao@moseley.ucsc.edu

The negative thermal expansion (NTE) observed in ZrW_2O_8 presents a unique opportunity to understand the interplay of Maxwellian underconstraint and symmetry incompatibility in anharmonic lattice-dynamics systems. Previous work showed that NTE in ZrW_2O_8 is driven by a set of modes of anomalously low energy. Here we use X-ray Absorption Fine Structure (XAFS) to elucidate the underlying wavefunction of these modes. Data were collected at both W L_{III}- and Zr *K*-edges to study the local structure around these two types of atoms. The data analysis shows that not only the local distortions around the nearest W-O and Zr-O bonds, but also the nearest W-O-Zr linkage have a very small temperature dependence. The much larger temperature-dependent local distortions of the nearest W-W and Zr-Zr atom pairs provide evidence that the low-energy modes that lead to NTE correspond to the correlated vibrations of the WO_4 tetrahedra and its three nearest ZrO_6 octahedra. These soft modes involve vibrations along four equivalent <111> axes. Since vibrations along different <111> axes are coupled in the cubic ZrW_2O_8 structure, the development of a softmode displacive transition is frustrated.

Zirconium tungstate (ZrW_2O_8) has attracted considerable attention recently due to its large isotropic Negative Thermal Expansion (NTE) properties over a wide range of temperature (from 0.3 K to 1050 K) (*1*). An explanation of this unusual behavior was first suggested by Pryde *et al* (*2*) in terms of the Rigid Unit Mode (RUM) model. In this model, the low-frequency rotations of rigid polyhedra were suggested to be the origin of NTE. Recently, optical phonons of extraordinarily low energy have been found in several experiments and these phonon modes appear to make important contributions to NTE (*3-6*). However, there is no direct evidence as to the precise vibrational modes of these rigid units that lead to NTE in ZrW_2O_8. Such information will help to answer the question *"why doesn't ZrW_2O_8 undergo a soft-mode transition?"* The low-frequency of the optical modes and the open structure of ZrW_2O_8 suggest such a transition might occur. Indeed, a close structural relative, ZrV_2O_7, exhibits a symmetry-lowering transition where its NTE vanishes, replaced by a lower-symmetry, positive thermal expansion state (*7*). The absence of such a transition in ZrW_2O_8 is a question of fundamental significance, and one of us has argued for it's connection to the problem of geometrical frustration in triangular magnets (*8*). We have used the X-ray Absorption Fine Structure (XAFS) technique to investigate the local structure in this material in detail, and from that we can extract some important information about these low energy vibration modes and therefore address the origin of NTE in this material.

As mentioned above, ZrV_2O_7, shows isotropic NTE when T > 373K. Korthuis *et al* attributed the NTE in ZrV_2O_7 to the transverse vibration of the central O atom in the middle of the O_3V-O-VO_3 group (*7*). A similar mechanism was proposed by Mary *et al* to explain the large isotropic NTE in ZrW_2O_8 (*1*). Although the structures of these two materials look similar (both contain polyhedra with shared corners), the RUM calculations for these two systems show that RUMs do exist in ZrW_2O_8 while there are no RUMs at all in the ZrV_2O_7 structure (*2*). The comparison of the vibrational density of states also shows that there are many more low-frequency modes in zirconium tungstate, therefore the mechanism for the NTE effects in ZrV_2O_8 and ZrW_2O_8 are qualitatively different (*2*).

The structure of ZrW_2O_8 lattice contains two types of polyhedra: WO_4 tetrahedra and ZrO_6 octahedra. Three corners of each WO_4 tetrahedron are shared with its three nearest ZrO_6 octahedra; the remaining unshared corner of each WO_4 tetrahedron is oriented along one of the <111> directions (*1,3*). There are two types of W sites (W_1 and W_2) and four types of O sites in this material. Each W atom has

four nearest O atoms. The average on each W site yields a distribution of W-O bond lengths from 1.7083 Å to 1.8066 Å. Similarly the six nearest O atoms around each Zr atom, three O_1 and three O_2, are at 2.0344 and 2.0946 Å respectively (*9*) (Table. 1). The nearest W-W distance is 4.1282 Å between the W_1 and W_2 pair along a <111> direction. The lattice constant, *a*, is about 9.1494 Å, which can be written as: $a = \sqrt{2}\, D_{Zr\text{-}Zr}$, where $D_{Zr\text{-}Zr}$ is the shortest Zr-Zr distance.

XAFS data at the W L_{III}- and Zr *K*-edges were collected as a function of temperature at the Stanford Synchrotron Radiation Laboratory (SSRL). The energy-space data were reduced using standard procedures (*10*) and the resulting *k*-space data were Fourier transformed to *r*-space to show the peaks that corresponded to different shells of neighbor atoms. The amplitude of the nearest neighbor W-O peak in *r*-space has almost no temperature dependence from 20 to 315 K (See Fig. 1), while the nearest Zr-O peak amplitude only changes slightly with temperature. This strongly supports the concept of rigid units for both the WO_4 tetrahedra and ZrO_6 octahedra, although, it is clear that the ZrO_6 octahedra are slightly softer. A more surprising result is that the W-O-Zr linkage is also quite rigid with almost no drop in amplitude from 20 to 160 K and only a small drop in amplitude (~25%) as the temperature is increased to 315 K. In striking contrast, both the shortest W_1-W_2 and the Zr-Zr atom-pair linkage are very soft and the *r*-space peak decreases rapidly with temperature. These results indicate that correlated vibrations of the nearest W_1-W_2 and Zr-Zr atom pairs play a more important role for negative thermal expansion than the transverse vibrations of the W-O-Zr linkage.

Quantitatively the width, σ, of the atom-pair distribution functions (PDF) provides information about local distortions, including thermal vibrations and static distortions. σ^2 is sometimes called the "Debye Waller factor" (*11*), and the slope of the σ^2 *vs.* T plot at high temperature is inversely related to the Debye temperature when acoustic phonons dominate the behavior. If optical modes dominate, an Einstein model is more appropriate for the thermal vibrations. σ can be extracted by fitting the *r*-space data to a sum of theoretical standards (*12*) calculated using the FEFF7 program (*13*). The nearly temperature independent plot of σ^2 *vs.* T for the nearest W-O bond (Fig. 2) indicates a very high Debye temperature and clearly shows that the WO_4 tetrahedra are rigid units over a wide temperature range (from 20 to 315 K). σ^2 for the

nearest Zr-O bond also changes little with temperature, which indicates that the ZrO_6 octahedra are quite rigid over this temperature range although slightly softer than WO_4. The local distortion of the W-Zr (Zr-W) linkage shows a small temperature dependence that is comparable to that of the nearest Zr-O bond. Such a small change in σ for the W-Zr pair over a fairly wide temperature range (5 to 315 K) is very surprising, and suggests that vibrations of the W-O-Zr linkage also have a high Debye temperature. σ^2 for the nearest W_1-W_2 atom pair shows a strong temperature dependence as does σ^2 for the nearest Zr-Zr atom pair. In addition, the temperature dependence of σ^2 for Zr-Zr clearly follows that of W_1-W_2, which is surprising.

One of the first proposals for the origin of NTE was that a large, low-frequency, transverse vibration occurs for the oxygen in the middle of the W-O-Zr linkage (*1*), as a result of the unconstrained corner of each WO_4 tetrahedra (*1-3*). If the O had a large transverse vibration, we would observe a large temperature dependence of σ^2 for the W-O-Zr linkage. Instead, this linkage is quite stiff, which means that a type of vibration other than a simple transverse mode for the O is involved in the low-energy vibration modes observed for ZrW_2O_8 in measurements of the specific heat and phonon density of states (*3-6*). Then, the principal unanswered question is: "*what is the vibrational wavefunction for those low-energy optical phonons which cause NTE in ZrW_2O_8?*"

The large changes in local distortion with temperature on the nearest W-W atom pair and the nearest Zr-Zr atom pair (Fig. 2) suggest that the vibrations between these two atom pairs have much lower energies than that for the W-O-Zr linkage, and therefore these vibrations should be considered as candidates for the origin of NTE.

Notice that the σ^2 *vs.* T curves for the nearest W_1-W_2 and the nearest Zr-Zr atom pairs behave quite similarly, which suggests some correlation between these vibrations; on the other hand, since the W-O-Zr linkage is quite stiff, it is not surprising that the motions of a WO_4 tetrahedra and its three nearest ZrO_6 octahedra are correlated. In a unit lattice cell of ZrW_2O_8, the two nearest WO_4 tetrahedra along a <111> direction are each surrounded by three ZrO_6 octahedra (all at face-centered sites). Each set of three

octahedra are in a plane perpendicular to the <111> axis, with one tetrahedron located in the center (on the <111> axis but slightly out of the plane) (Fig. 3: A). A simple rigid -tentpole-model is used to explain the correlated motions of W and Zr(Fig. 3: B). Consider the W atom to be at the top of a small triangular tent with rigid poles connected to the three Zr atoms on the ground. If the W is raised, then the base area must shrink due to the three rigid legs. The lattice constant of the zirconium tungstate is the distance between the second nearest Zr -Zr atom pair, which is $\sqrt{2}\ D_{Zr\text{-}Zr}$. As the temperature increases, the nearest Zr -Zr distance will on average become shorter due to the increased vibration of the WO_4 along a <111> axis; thus we expect to have a lattice contraction. Since there are four equivalent <111> axes, such contractions should occur in all directions.

However why can't one of these modes sof tens and lead to a soft -mode displacive transition? From a theoretical p erspective, there would be four equivalent modes (per cubic unit cell) along each of the possible <111> axes. However, such a four -fold degeneracy is inconsistent with cubic symmetry a nd the actual eigen -modes must therefore be linear combinations of the observed <111> displacements along different axes. This implies that the motion of the W and Zr for vibration of the W along a given <111> axis are coupled to other <111> axes. This frustrates a possible soft-mode transition.

The coupling between different axes can be understood from a detailed examination of the structure. Fig. 4 shows a plane of the crystal, perpendicular to the <111> axis; Zr atoms are at the corners of each triangle, W atoms are black or gray dots and O atoms have been omitted for clarity. Note that the structure contains both filled triangles (with W atoms in the center) and non -filled triangles. Six non -filled triangles form a hexagonal structure. If the filled Zr triangles contract as the W atoms vibrate transversely, the Zr hexagon must either contract or the central Zr atom will have to move out of the plane a distance $\sqrt{3}$ times the W displacement. The later is not possible due to constraints on the Zr. Since each side of a non -filled triangle in the hexagon is one side of a *filled* triangle in another plane (perpendicular to a different <111> axis), a contraction of the Zr -Zr distances inside the hexagon will drive vibrations along each of the other three <111> axes.

In conclusion, the WO_4 tetrahedra and ZrO_6 octahedra were found to be rigid units over a wide temperature range (5 to 350 K) as suggested by other experiments. However, the linkage of these two types of polyhedra is also quite rigid ($\sigma_{W\text{-}Zr}$ increases very slowly with T) over this temperature range, which results in a correlated vibration between the nearest W and Zr atom. Such a large rigid unit consisting of several polyhedra is very surprising. The correlated motions between the WO_4 tetrahedra and ZrO_6 octahedra provide an explanation for the large unusual negative thermal expansion in zirconium tungstate. Such correlated motions also frustrate the formation of a soft-mode transition; the lattice shrinks uniformly along all four <1 1 1> axes, which maintains the cubic lattice structure. Note that the small temperature dependence of $\sigma_{W\text{-}Zr}$ means that the transverse vibrations of O in the W-O-Zr linkage cannot be large and hence cannot be the primary origin of NTE in this material.

REFERENCES AND NOTES

1. T. A. Mary, J. S. O. Evans, T. Vogt, A. W. Sleight, *Science* **272**, 90 (1996).
2. A. K. A. Pryde *et al*, *J. Phys.: Condens. Matter* **8**, 10973 (1996).
3. A. P. Ramirez, G. R. Kowach, *Phys. Rev. Lett.* **80**, 4093 (1998).
4. G. Ernst, C. Broholm, G. R. Kowach, A. P. Ramirez, *Nature* **396**, 147 (1998).
5. W. I. F. David, J. S. O. Evans, A. W. Sleight, *Europhys. Lett.* **46**, 661 (1999).
6. R. Mittal, S. L. Chaplot, *Solid State Communications* **115**, 319 (2000).
7. V. Korthuis *et al*, *Chem. Mater.* **7**, 412 (1995).
8. A. P. Ramirez, in *Handbook of Magnetic Materials*, K. H. J. Buschow, Ed. (North Holland, Elsevier Science B.V., Amsterdam, The Netherlands, 2001), Vol. **13**, pp. 423-520.
9. J. D. Jorgensen *et al*, *Phys. Rev. B* **59**, 215 (1999).
10. First, the energy-space XAFS data (μt *vs.* X-ray energy, E, plot, where μ is the absorption coefficient and t is the sample thickness) were collected in SSRL. Then a pre-edge subtraction was applied to remove the absorptions from other edges. We fit a five-knot spline to the post-edge XAFS data to determine the background function μ_0 and thereby extracted the XAFS function, χ, which is defined as $\chi = \mu/\mu_0 - 1$. The k-space data, which is normally plotted as $k\chi$ *vs.* k (k is the wave vector), were then Fourier transformed to real-space. Each peak in real-space corresponds to a certain atom-shell with a well-defined phase shift and pair distribution function, which indicates how atoms in that shell are distributed around the central (absorption) atom. $k^3\chi$ plots were used for the W L_{III}-edge data in order to show the XAFS data at longer distance better.

11. σ is a broadening factor of each peak in real -space XAFS data. We can extract information about the local distortion of a particular atom shell around the central atom from the σ. A Gaussian pair distribution function was used to fit each atom shell in the real-space data, from which σ is determined.

12. The theoretical standard for the nearest W -O peak is an average of the functions generated for each of the short W -O distance from 1.71 to 1.81 Å. Four distances within 0.1 Å cannot be resolved by the XAFS technique. The theoretical standard for the nearest Zr-O peak is also the average for two nearest Zr-O distance: 2.03 and 2.09 Å for the same reason. Both W-Zr (Zr-W) single scattering and W-O-Zr (Zr-O-W) multiple scattering effects were considered to obtain the theoretical standard for the nearest W-Zr (Zr-W) peak. XAFS cannot differentiate between W_1 and W_2, so we have to average the theoretical standards of both W sites. The same procedure was applied to get the nearest W-W theoretical standard. We carried out another fit, which fits the single and multiple scattering peaks separately, and it shows that σ is about the same for both contributions.

13. S. I. Zabinsky, A. Ankudinov, J. J. Rehr, R. C. Albers, *Phys. Rev. B* **52**, 2995 (1995).

14. This work was conducted under the auspices of the U.S. Department of Energy (DOE) and was supported by NSF grant DMR0071863. The experiments were performed at SSRL, which is operated by DOE, Division of Chemical Science, and by the NIH, Biomedical Resource Technology Program, Division of Research Resources.

Table 1. Selected atom -pair distances and degeneracy calculated from neutron powder -diffraction data at room temperature (300 K), reported by Jorgensen *et al*[9].

Atom Pair	Degeneracy	Distance (Å)
$W_1 – O_1$	3	1.8066
$W_1 – O_4$	1	1.7083
$W_1 – O_3$	1	2.4103
$W_2 – O_2$	3	1.7852
$W_2 – O_3$	1	1.7178
$W_1 – Zr$	3	3.7452
$W_2 – Zr$	3	3.8697
$W_1 – W_2$	1	4.1282
$Zr – O_1$	3	2.0344
$Zr – O_2$	3	2.0946
Zr – Zr	6	6.4554
Zr – Zr	6	6.4839

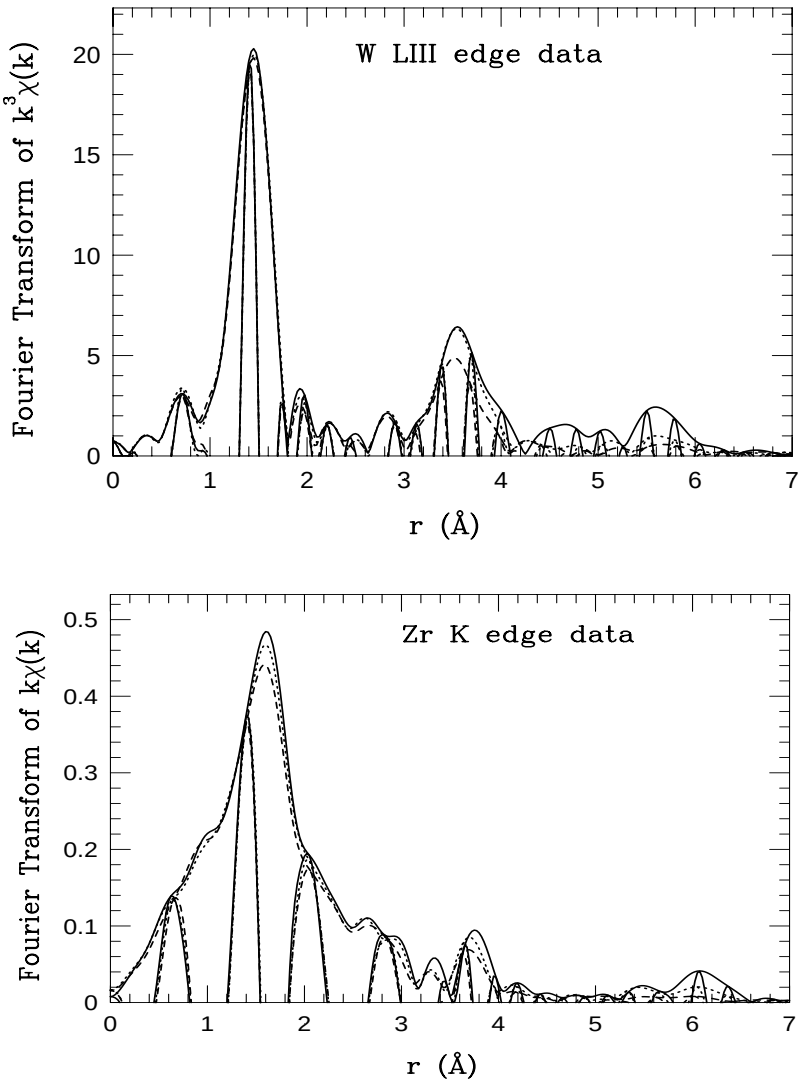

Fig. 1. Plot of XAFS real-space data for both W L_{III}- and Zr *K*-edge data up to 7 Å. Data at 20 K (Solid line), 160 K (dotted line) and 315 K (dashed line) are shown for each edge. The Fourier Transform range is from 2.8 to 14.0 $Å^{-1}$, with 0.3 $Å^{-1}$ Gaussian broadening. The high frequency curve inside the envelope is the real part of the Fourier Transform (FT_R). The envelope is defined as $\pm\sqrt{FT_R^2 + FT_I^2}$, where FT_I is the imaginary part of the Transform. There is a well-defined XAFS phase shift for each peak, consequently the nearest W-O peak occurs at ~1.4 Å (upper panel), the nearest W-Zr peak (including W-O-Zr linkage) shifts to about 3.5 Å and the nearest W-W peak is around 3.9 Å. In the bottom panel, the nearest Zr-O peak is at 1.6 Å; the nearest Zr-W peak (including Zr-O-W linkage) shifts to about 3.75 Å; the nearest Zr-Zr peak is around 6.0 Å.

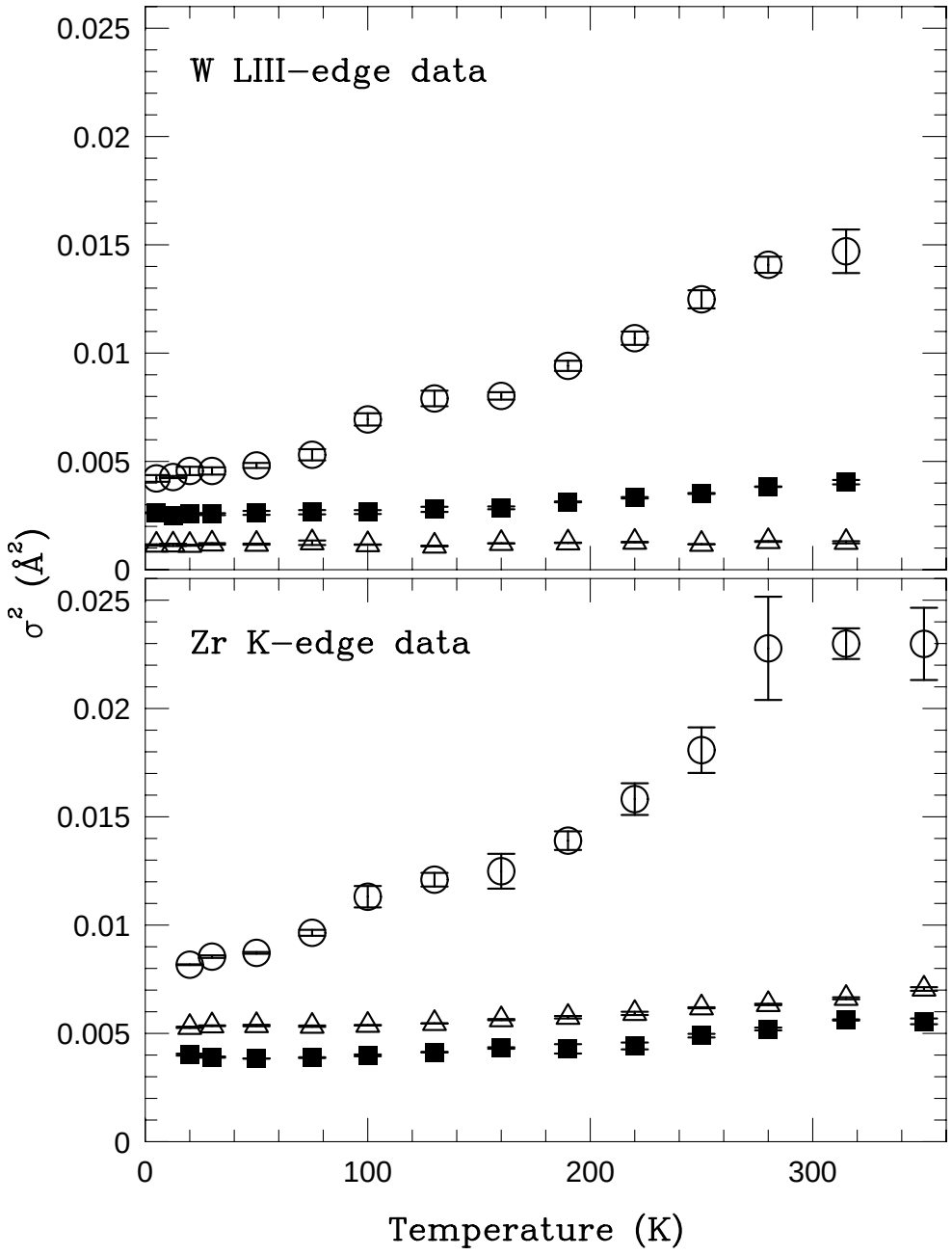

Fig. 2. Plot of σ^2 *vs.* temperature. In the upper panel, which shows the W L_{III}-edge data, the open triangle s represent the nearest neighbor W-O bonds; the solid square sh ows σ^2 for the W-Zr pair including W-O-Zr multiple scattering effects; the open circle represents the nearest W $_1$-W_2 atom pair. In the lower panel, σ^2 for three atom pairs are shown: the nearest neighbor Zr-O bond (open triangle), the nearest Zr -W pair including the Zr-O-W linkage (solid square) and the nearest Zr-Zr pair (open circle).

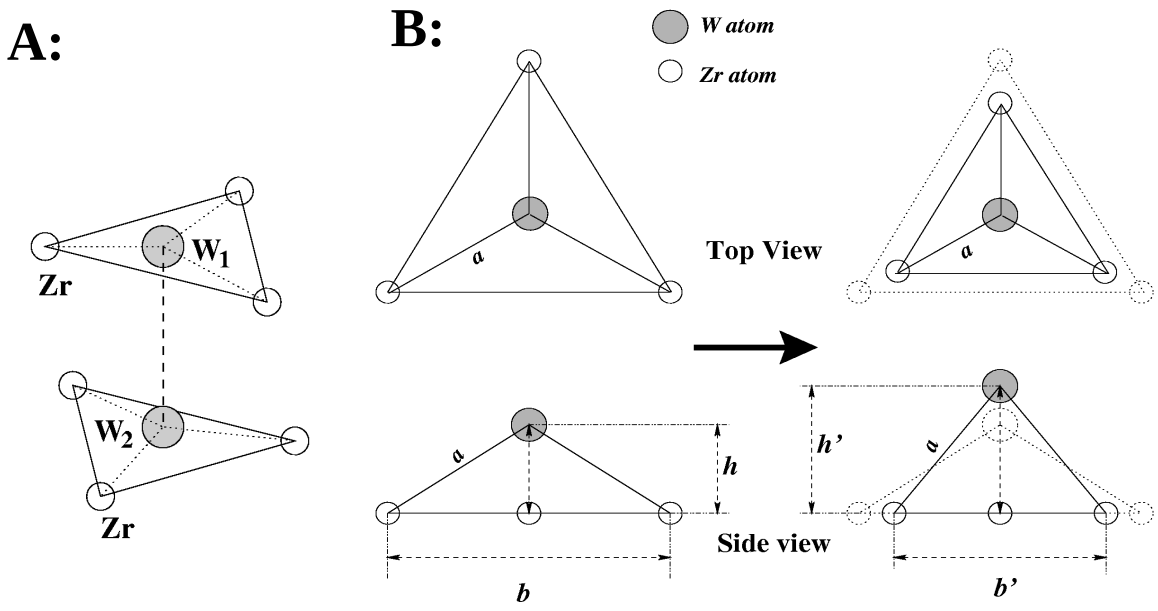

Fig. 3. (**A**) A simplified drawing of part of the structure which shows three nearest Zr atoms in a triangle surrounding either the W_1 or W_2 atoms. (**B**) A rigid-tentpole-model to show the constraint on the correlated motions between a W atom and it nearest Zr atoms. As W moves up (right side of the figure) , the Zr must move together to keep the W-Zr linkage rigid. This leads to a net lattice contraction.

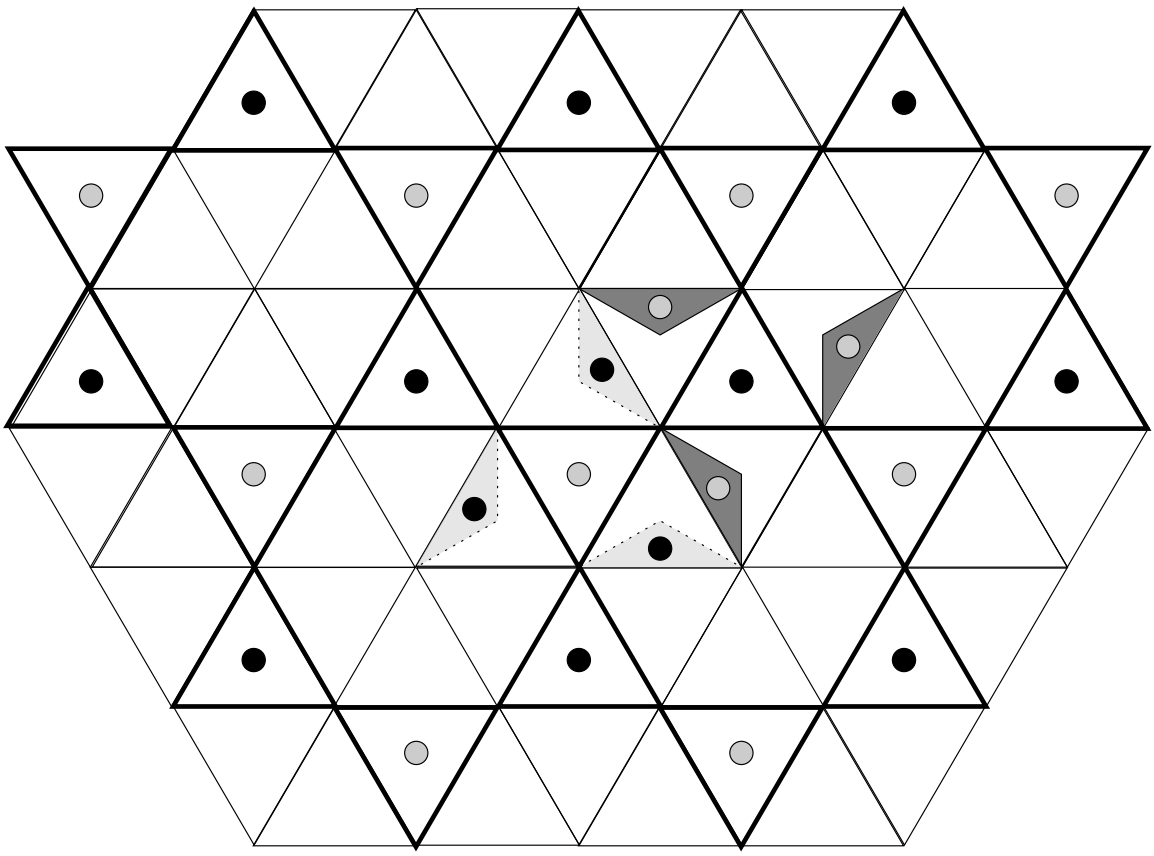

Fig. 4: A sketch of the plane perpendicular to a <111> axis. Only the framework of Zr and W is shown here. Zr atoms are at the corners of each triangle, while each W atom is at the center of every thick -line triangle. The gray and black circles are W_1 and W_2 respectively. The six shaded small triangles (three light gray and three dark gray) are not in the plane, but correspond to triangles in planes perpendicular to other <111> axes. Here the light gray triangles have one vertex below the plane, while the dark gray triangles have a vertex above the plane.